Investigation into MoTe2 based Dielectric Modulated AMFET Biosensor for Label-free Detection of DNA including Electric Variational Effects

Arpan De (arpantukan@gmail.com)
Jadavpur University https://orcid.org/0000-0002-2991-5293
Sharmistha Shee
Jadavpur University
Subir Kumar Sarkar
Jadavpur University

Research Article

Keywords: Deoxyribose Nucleic Acid (DNA), Biosensor, DMFET, Transition metal dichalcogenides (TMD), Circuit Analysis

Posted Date: July 8th, 2021

DOI: https://doi.org/10.21203/rs.3.rs-676562/v1

Version of Record: A version of this preprint was published at Silicon on October 15th, 2021. See the published version at https://doi.org/10.1007/s12633-021-01423-7.

Abstract

Due to limitations of Silicon, Transition metal dichalcogenides (TMD) based biosensors are popular in the recent times. In TMD family, Molybdenum telluride (MoTe2) is being studied a lot for different biosensing application. However, for DNA detection using TMD based DMFET, the effect of the electrical variations in DNA has not been studied before. Also, the impact of DNA-Electrode interaction on transducer level of DMFET is yet to be studied. In this article, we have proposed a Molybdenum telluride (MoTe2) based Accumulation Mode Field Effect Transistor (AMFET) for possible dielectric modulated biosensing application. The study is focused on DNA detection including the electric variations of DNA due to surface interaction. We have done a circuit level analysis of the proposed structure for having deeper insights into its performance under various DNA orientations in the nanogap. We have also presented a benchmarking to highlight the superior sensitivity of the proposed structure (ΔVth = 700mV at K =8). The impact of back-gate bias is also included. We have obtained significant variation of threshold voltage shift for different orientation in the proposed structure suggesting strong impact of electrical variations in DNA in biosensing performance of MoTe2 AMFET.

1. Introduction

To serve a larger spectrum of humanity, biosensors have been evolved and enabled for label-free detection in the arena of agriculture, medicine, ecological surveys, food industry, etc. [1, 2].The reason behind the popularity of label-free biosensors is its immediate response capability for bio-analyte identification without complex probe arrangements. A large amount of research has been done on biosensors for the detection of proteins, viruses, and DNA [3–10].

Ion-sensitive Field Effect Transistor (ISFET) was the most trivial biosensor which was proposed a long way back. Its performance is exceedingly well in the case of charged molecule detection. However, the neutral molecule detection is not so overwhelming in the case of ISFET [11] In comparison to (ISFET), which on the charge interaction effect, Dielectric Modulated Field-Effect Transistors (DM-FET) are capable of detection of non-charged biomolecules & thus have a wider perspective. Widescale research has been carried on DMFET biosensors for years [3–10]. While some studies focus on increasing the sensitivity of DMFET biosensors, others emphasized unveiling the underlying physics of such label-free biosensors. FET biosensors work on two principles i.e., (i) charge interaction and (ii) dielectric constant modulation effects. The biomolecules immobilize inside the craved cavity in DMFET, modulates the effective oxide capacitance, and consequently, effective dielectric coupling between gate & channel varies. Changes in electrical properties quantify the sensitivity for label-free detection for both neutral & charged molecules viz. biotin-streptavidin & DNA [3–10]. The approach played a vital role in making DMFET widely explored structure for label-free biosensors with inherent advantages like higher sensitivity, power consumption, higher scalability & fabrication simplicity.

In keeping with the advancement in semiconductor technology, the research aims for smaller FET Biosensors with a higher density as well as higher sensitivity [12]. At biosensor cavity thickness touching

sub-10 nm regime, several research works are focusing on FinFET & nanowire FET for detection of DNA, Proteins, viruses, etc. [13]. At scaled dimensions, Silicon-based FET biosensors are found to be inadequate to provide crucial sensing performance metrics. After isolation of graphene in 2004, research works in ultra-scaled DMFET biosensor has been flourishing based on TMD (MoS2, MoSe2, WS2, WSe2 etc.) material. The atomic thinness along with a higher surface/volume ratio results in a stronger response to surface adsorption phenomena & makes TMDs the best-suited material for sensing applications [13]. In addition, denser active surface sites, broader & tenable electronic properties (due to layer-dependent band structure), enhanced selectivity to specific analytes & extremely high sensitivity opens up the endless opportunity for TMD-DMFETs to be next-generation scaled biosensors for particularly for healthcare applications [14]. For detection of DNA (exceedingly important for medical research, cancer diagnostics, forensics, etc.), the traditional process of preamplification & optical detection (i.e., measurement of fluorescence intensity of labeled strands, etc.) demands specialized infrastructure & human resources [14]. Here, TMD-based DMFETs for DNA electrochemical detection emerged as a cost-effective, speedy detection method that too with a much lower detection limit in the range of Femto- or attomolar. Detection of different DNA strands by 2D-DMDFETs has been explored by researchers viz. Jin et al. on Dengue DNA using graphene oxide and wrapped SiO2 particles. Zhang et al. for tumor DNA. using exfoliated MoS2, Checkin et al. for HPV DNA, using graphene oxide (prGO)/MoS2 composite [13]. The linear range & detection limit of the last cited research has been reported 3.5 – 35.3 pM, and 1.75 pM respectively [15]. Very recently, Hwang et al. has reported crumpled graphene 2D material-based FET biosensor with ultrasensitive detection of DNA and RNA molecules with significantly low limit of detection (LOD) [16].

For more advanced applications, MoTe2 is being considered suitable material for biosensor 2D material-based DMFETs due to a smaller bandgap, lower thermal conductivity with a higher Seebeck coefficient when compared with other 2D materials [17]. In addition, MoTe2 showed unique & viable properties in the TMD family in terms of growth, bandgap engineering, carrier injection, etc. [17]. A high ratio of on/off current with low subthreshold swing made the MoTe2 one of the most suitable candidates for a device, logic circuits, optoelectronics as well as sensing application. Recently, Feng et al. reported a high sensitivity of molybdenum ditelluride ($MoTe_2$) sensor with a significantly improved recovery rate [18]. In literature, it has been widely reported that experimental results underperform theoretical prediction due to irregular arrangement of biomolecules in the

cavity, steric hindrance effect, partial hybridization & weak binding possibility, probe- arrangement variability, etc. [19]. As these lead to significant performance degradation, the

minimum detection limit becomes a vital performance parameter in addition to sensitivity in the scaled regime .

In this manuscript, we have proposed a $MoTe_2$ based Accumulation Mode Field Effect Transistor (AMFET) for biosensing application. In the following sections, we have mainly focused on understanding the $MoTe_2$ based biosensor performance for DNA detection. A general sensitivity analysis of the

proposed structure has been presented at the beginning and the device performance has been benchmarked with previously reported DM-MOSFET studies. The impact of the interaction between the DNA strands and gate electrodes is one of the experimentally validated sources of variability. The effect of electrical variations in DNA due to interaction with electrode on the performance of biosensors is studied in detail. We have also considered the effect of irregular orientations of DNA on biosensor performance in form of case studies. The study has been conducted on both device and circuit levels.

2. Device Structure And Simulation Methodology

$MoTe_2$ Accumulation Mode Field Effect Transistor is proposed as the device under analysis. The channel height is taken to be 10 nm. The channel length is 35 nm. Source and Drain extensions are 20 nm each. A SiO_2 box is considered of height 10 nm as well. Cavity height is kept constant at 10 nm. A small portion of SiO_2 is considered for the immobilization of biomolecules. The top and bottom gates are considered to be Gold(Au) with work-function 5.1 eV. Source and Drain regions are doped heavily with concentration of 10^{20} /cc (n-type), while the channel region is doped very lightly with concentration of 10^{16} /cc (n-type). The detailed schematic of the device structure can be found in Fig. 1.

The proposed AMFET has been simulated using SILVACO TCAD [20]. The study has been done on two levels. The first is the device level analysis and the second one is the circuit level assessment. For the first set of studies, we have adopted Fermi-Dirac statistics as the main carrier statistics. When the device is in thermal equilibrium, carriers seem to obey Fermi-Dirac statistics with the semiconductor lattice [20]. For mobility, we have adopted the Concentration-dependent mobility model and Field Dependent mobility models for capturing mobility variation under high electric fields. Lombardi mobility model have been taken into consideration to account mobility degradation effect at the inversion layer due to the high surface scattering phenomenon. Shockley-Read-Hall recombination model is included. Since the source and drain are highly doped regions, there will be significant band bending in these regions due to high doping. To include this in calculations, Bandgap narrowing effects have also been taken into account. Quantum effects has not been included as quantum confinement plays major role in sub-10 nm domain and this work has been done with channel thickness 10 nm. All the models mentioned above along with a drain voltage of 0.5V (for low energy operation) is deployed to obtain the DCIV characteristics of the proposed architecture and other device level parameters like threshold voltage etc.. Our simulation setup is well calibrated and shown in Supplementary File. For the second set of studies i.e., circuit level assessment the proposed structure along with the model mentioned above are fused into the MIXEDMODE package of SILVACO ATLAS [20]. Both DC and Transient simulations using the above structure is done for different levels of analysis to explain the device behavior in details.

The proposed structure is intended to perform as Dielectric Modulated Biosensor. For simulating different biomolecules,

the electrical properties of the nano-particles are taken in to considerations. The cavity dielectric constant is varied in regard of different biomolecules (neutral). For charged biomolecules, the effective charge

effect is being considered in form of the interface traps at the cavity and channel interface. For circuit simulations as well, this methodology has been followed.

3. Benchmarking

In this manuscript, we have mainly focused on understanding the biosensor performance for detecting the DNA biomolecules, which are charged in nature. However, to establish that this proposed biosensor offers superior sensitivity for neutral biomolecules as well, we have presented a benchmarking with the already reported Silicon based biosensor studies in Fig. 2. The data for low dielectric constant (K = 2) and high dielectric constant (K = 8) based biomolecules are presented in the above figure. We can witness that the proposed $MoTe_2$ based AMFET outperforms other Silicon based biosensors for both high and low dielectric constant based biosensors. It is to be noted that for benchmarking purpose, we have not considered the DNA variability as the previous studies do not include this factor.

4. Results And Discussion

In the following sections, we have presented various analysis both on device level and circuit level for understanding the DNA detection capability of proposed structure and also the way, performance is hampered by variability sources. The sensitivity of a parameter Q_1 is calculated following the equation:

$$Sensitivity\ (S_{sen}) = \left|\frac{Q_1(\rho=c) - Q_1(K=1)}{Q_1(K=1)}\right| \quad (1)$$

The term $K = 1$ stands for the bare device condition i.e., the cavity is not-filled with any biomolecules or linkers. ρ stands for the charge density of the biomolecules. $\rho = c$ means charge of a particular molecule is c. Another important study is the selectivity. The selectivity of a parameter Q_1 for one condition u_1 with respect to other u_2, is calculated by the following the equation:

$$Selectivity\ (S_{sel}) = \left|\frac{Q_1(u_1) - Q_1(u_2)}{Q_1(u_2)}\right| \quad (2)$$

These equations are used for all the sensitivity and selectivity study done in the upcoming sections. For the study without DNA-Electrode Interaction Effect, we have considered conventional approach while for that including DNA-Electrode interactions we have relied on experimental setup as mentioned in [22-24].

A. DNA Detection without considering DNA-Electrode Interaction

As mentioned in [21], monolayer of ssDNA (single-stranded DNA) is genetically coded in to the cavity which serves as the base for DNA hybridization. This base layer is particularly efficient in binding with a specific target DNA strands which results in high selectivity in target detection. This step is shown in Fig. 3b. The DNA next hybridize with this base layer after immobilization to form dsDNA. After sometimes, the number of full hybridized dsDNA increases and we get the cavity fully filled with DNA biomolecules. In

order to have deeper insight into the transition from partial to complete hybridization of DNA we have analyzed one of the intermediate stages of partial hybridization as shown in Fig. 3c. Fig. 3d shows the completely hybridized cavity. From a simulation point of view, each of the stages as shown in Fig. 3 and discussed above is associated with definite dielectric properties. The details of the dielectric constant and charge of each layer is provided in the Supplementary File.

With drain voltage (V_{ds}) of 0.5V and back-gate at zero bias condition, the top-gate bias (V_{TG}) is varied up to 4V to get Current-

Voltage characteristics of the proposed biosensor during the four stages of DNA detection. For bare device, i.e.,

when cavity is filled with air, the gate capacitance is the least. Consequently, electric coupling between the gate electrode and semiconductor lattice is worst. As a matter of fact, a smaller number of electrons are pulled towards to surface to form the conduction channel which results in very low current. Also, less gate controllability over channel, causes comparatively higher OFF Current as can be seen in Fig. 4(a) (Dark Blue). Now as ssDNA base layer is formed in the cavity, the channel conduction increases due to improvement in gate-channel coupling which presents a better current profile. As we transit from partial to complete hybridization, the effective gate capacitance increases which results in higher I_{ON} and lower I_{OFF}. All features can be seen in Fig. 4(a). From a biosensor perspective, the sensitivity and selectivity of different stages are important. As can be observed in Fig. 4(b), the current sensitivity is very high for Completely hybridized stage in comparison to bare device. The max Current sensitivity is about 10^5 for Completely hybridized stage, which it is 10^4 and 10^2 for partially hybridized and ssDNA stages respectively. In order to differentiate between the different stages, we have analyzed the selectivity as well. From Fig. 4(c), we find the selectivity of fully hybridized stage is approximately $7x10^4$ and 100 with respect to ssDNA stage and partially hybridized stage and a reduction of almost 61% can be seen in between these two cases. Thus, we may conclude that $MoTe_2$ based AMFET can differentiate between levels of DNA detection with a good level precision. The Threshold sensitivity is also much higher for completely hybridized DNA stage (approx. 0.29) in comparison to 0.14 and 0.21 in case of ssDNA and partially hybridized dsDNA respectively.

B. DNA Orientation Effect and Implementation Methodology

The immobilization of DNA plays an important role in biosensing performance. Specifically for DNA biosensors, the interaction of DNA with surface is a vital factor for DNA genome sequencing or biosensing. Several researches have been carried out over the years to understand the characterization of DNA when it comes in contact with surface [22-24]. Among others, some noteworthy problems associated with single molecule systems like DNA are their orientation, biological affinity, electrode surface status under microenvironment and so on. In addition to these, previous studies [23,24] have reported altercation in DNA electrostatic characterization also controls the nature of interaction with surface. As mentioned in [23,24], the way DNA interacts with

gold surface is greatly affected by the electrostatic variations, precisely the orientation of DNA present on them. If the applied bias exceeds the potential of zero charge (PZC) for any electrode, then we will witness such variability in DNA orientation [22,24].

The potential of zero charge is defined as the potential value at which net charge density comes to zero on the electrode surface. This PZC depends on several factors like concentration of solution, microenvironment of the electrode and so on. Hence, the concept can be extended to any electrodes, provided its surface interaction with DNA is well verified. Since, we have experimental evidence for gold electrode (PZC = 0.26 V), we have considered gold to be gate electrode in our simulations as well. In Fig. 5, we have presented a schematic of different orientations a DNA can have in course of its interaction with the gold surface. The brown arrows show the electric force of attraction of the gate electrode. Others forces working on the single molecule system, DNA are the mutual repulsive force (as DNA negatively charged in nature) and the repulsion from the

majority carriers in the semiconductor lattice (as it is n-type; for p-type there would have been attraction). For our simulation purpose, we have considered a self-assembled monolayer mainly consisting of thiol linkers. The value of relative dielectric constant of the layer is considered '2' [22]. The length of DNA strands is considered to be 7nm and relative dielectric constant of 8. The inter-strands distance is 2nm. It has been reported in [22,23], that double stranded fully hybridized DNA strands can be considered to be rigid rods with homogenous charge distribution over them. Hence, we have considered, if the COM of the DNA leans by an angle of Θ with respect to the SAM layer, both the strands of DNA will incline at a same angle. This approximation is a valid one as reported in [22]. In the following sections, we shall see the effect of this variability in details from device and circuit perspectives.

C. DNA Orientation Effect – Device Level Perspective

A large variation in the potential profile and electron distribution can be seen for DNA oriented vertically and horizontally in Fig. 6. This level of variation has significant effects on the device performance as can be seen in Fig. 7. In Fig. 7, we have presented the 'Current Sensitivity' and 'Threshold Sensitivity' of the proposed $MoTe_2$ based architecture which are important from biosensor performance. The Id-Vgs profiles for each of these different orientations are provided in Supplementary Material. In Fig. 7(a), the sensitivity of the vertical position is about $6x10^3$ while that for horizontal is almost 1. Sensitivity above 1 is considered appreciable. The reason for such a low sensitivity of horizontal position is that the amount of gate coupling increased due to 2nm addition of DNA strands is not sufficient to cause appreciable amount of current conduction. Sensitivity for 45^o inclination of DNA strands is $1x10^3$ which is 6 times less than that for vertical position. From Fig. 7(b) the threshold sensitivity is very high for vertical or near vertical positions but they decrease as DNA inclines more and more towards the SAM layer. Threshold sensitivity for vertical position is about 4 times more than that of horizontal one. Hence, we can safely say the orientation of DNA has significant impact on the biosensing performance.

D. DNA Orientation Effect – Circuit Level Perspective

D.1. DC Simulations

For the circuit level assessment, we have considered a resistive-load based NMOS inverter as shown in Fig. 8. The source end of the biosensor is always kept grounded. The drain is connected with the resistive load of 100KΩ which in-turn is connected to a DC voltage source of value 2.5V. In the biosensor architecture, there are two nodes at which inputs are given. The top-gate is the main node here. V_{TG} is considered to be a constant value for DC simulations and it is in form of a pulse for Transient simulations. The back gate voltage is constant at a definite value for both DC and Transient simulations. The output taken out from the drain of the biosensor. However, the back-gate bias value has been changed and its effect on biosensing performance is discussed in next sections. For DC analysis, we have presented the biosensing performance in terms of 'Voltage Transfer Characteristics', 'Output Voltage Selectivity', 'Input-High (V_{IH})' and 'Input-Low (V_{IL})' voltage selectivity.

The voltage transfer characteristics in Fig. 9(a) shows the inverter performance with vertical orientation is better than all other orientations. The reason is the better opportunity of gate coupling in case of vertical orientation as can be seen from the above device level studies. In order to have insights on comparative performance of different orientations, we have plotted the output voltage selectivity curve with respect to the vertical orientation in Fig. 9(b). We can witness a high selectivity for the horizontal orientation. A peak selectivity of 50 for horizontal position and 32, 20 and 5 for 15^o, 30^o and 45^o respectively. In Fig. 9(c), in terms of selectivity of Input-High (V_{IH}) and Input-Low (V_{IL}) voltages, we can see 0.5 (average) selectivity for horizontal position with respect to the vertical position. Thus, we can conclude that the $MoTe_2$ based biosensor can successfully differentiate between the horizontal

and vertical orientation of the DNA in the nanocavity. Also, it is important to notice that the DNA interaction plays a very important role in biosensing performance which is presented further in the next sections.

D.2. Transient Simulations

In the previous paragraph we have studied the circuit performance in case DC simulation. In this paragraph, we shall be discussing about the transient simulation results. In Fig. 10(a), Input-Output voltage curve is plotted. It can be seen that there is distinctive difference in the characteristics for horizontal and vertical positions. The difference is so significant that it can easily be measured with any voltmeter. The same can be said for the Current-Voltage profile as well in Fig. 10(b). The vertical position shows a very steep switching whereas the horizontal position due to lack of enough channel controllability of the gate has very slow switching. Any intermediate orientation angle is to have characteristics in between the red and blue curves shown in Fig. 10 (a) and (b). Thus, from transient simulations as well one can easily decipher the orientation of the DNA in nanocavity. The propagation delay has been calculated by considering the average of rise-time delay and fall-time delay.

For propagation delay selectivity, the delay in case of vertical orientation is compared with that of other orientations. The propagation delay of the inverter for all orientation angles are is shown in Fig. 10(c) and the selectivity of them with respect to vertical orientation is shown in Fig. 10(d). The delay decreases from horizontal to vertical orientation suggesting faster switching in case of higher orientation angles. For horizontal orientation, the cavity is mostly covered with air. As a result, the gate coupling could not form the inversion channel for easy conduction of current in the AMFET. As a result, significant delay can be noticed in this case. However, in case of Vertical Orientation the delay decreases by almost 1.3ns due to improved channel formation. Due to this high variation of gate coupling effect in both these cases, we see a selectivity of about 20 for horizontal case with respect to vertical one. The complete transient profile for Output Voltage and Output Current can be seen in Fig. 10(e) and 10(f) respectively, where both switching and delays can clearly be seen.

E. Impact of Back-Gate Bias

For all the analysis, until this point, the back-gate bias has been considered to be zero. However, for a holistic study of DNA detection with $MoTe_2$ AMFET, the study for the effect of back gate bias is really important. In Fig. 11(a) it can be seen that with V_{BG} = 1V, the electron concentration in the channel increases and becomes more uniform when compared to Fig. 6 (c,d). The reason is that higher back-gate bias causes more majority carrier influx into the channel which results in higher electron concentration near the surface. Also, it reduces the impact of top-gate over the channel as for both horizontal and vertical orientation, electron distribution is more or less same. Thus, qualitatively, it reduces the sensitivity of the proposed biosensor. For quantitative explanation, we can see Fig. 11(e,f). In previous section, we discussed the significant difference for Output Voltage and Output Current between horizontal and vertical cases can help us to determine the nature of DNA interaction with surface. But with increased back-gate bias, both switching and delay of the adopted NMOS architecture are nearly equal due to availability of more electrons at the surface and reduced impact of top-gate. As a result, we cannot understand the DNA interaction nature for increased back-gate bias. Transient Current and Voltage Outputs are provided in Fig. 11(c,d). The impact of back-gate bias on the biosensor sensitivity from a device level is also studied and provided in details in the Supplementary File (Fig. S3,S4,S5). A degraded sensitivity is observed from device level perspective as well.

F. Variation of Biosensor performance for irregular orientation of DNA

In the previous section, we have analyzed the effect of DNA orientation based on an implicit assumption that all the DNA strands have the same level of orientation. Because of this reason, we have considered the DNA layer-end to be flat line. In real time experiment, there are many factors that causes hindrance in achieving this flat line of DNA layer. The steric hindrance causes the DNA to be non-uniformly placed which will prevent all the DNAs to be under same influence of gate voltage. Again, the initial layer of DNAs near the electrode shields the gate voltage for other layers. These factors together cause non-uniform degree of rotation for all DNAs. Thus, for having deeper insights into these non-uniform orientations, we have done some case studies. In Case A, Case B and Case C, the maximum height of

DNA layer is 7nm while for Case D, Case E and Case F is 3nm. For Case A and D, the peak DNA layer is near source while for Case B and E, the peak near to the middle of the channel and for last set of cases, the peak near to the drain effect. In Fig. 12(TOP) the potential profile of the channel for each of the cases are shown. It can be seen that potential profile is highly varying in case larger peak height of DNA layer in comparison to that with smaller peak height. It can also be witnessed from the above plots that as the peak position changes from source end to middle to drain end, the potential profile changes considerably, especially for larger peak height. Out of these three positions, when the peak is at the middle, the potential distribution over the channel is more uniform than the others. Thus, we expect the device to have better performance in this case in comparison to the other ones. Again, when the peak position is near the drain, the surface potential is higher than the rest of the cases. Higher surface potential suggests higher electron concentration near the surface which refers to higher current conduction. It can also be noted that for lower peak height, the peak position has very less effect on the potential profile. The reason can be attributed to the less channel controllability of the gate.

In Fig. 12(BOTTOM), the threshold voltage selectivity has been plotted with different peak position for different peak heights. As discussed above, for low peak height i.e., the cases with t_{peak} equal to 3nm, the threshold voltage selectivity change for different peak position is very nominal as the value centers round 0.1. The selectivity variation increases as we move towards higher peak heights. For t_{peak} equal to 5nm, the selectivity is 0.13, 0.11 and 0.198 for L_{peak} equal to 5nm, 15nm and 30nm. This variation increases much higher in case t_{peak} equal to 7nm. The reason is for higher peak height, a slight change in DNA position,

causes large amount of gate capacitance changes which is lower in case of low peak height. From Fig. 12(BOTTOM), it should also be noted that the selectivity is higher for drain side peak position as the higher electron concentration in the surface in this case results in higher current. This has been supported by the potential distribution in Fig. 12(TOP) (c).

5. Conclusion

In this manuscript, we have proposed a $MoTe_2$ based AMFET for dielectric modulated biosensing performance. We have specifically studied the DNA detection including the DNA-Electrode interaction effects. For our study, the DNA interaction with gold surface has been taken into consideration which is experimentally proven. We have noticed that significant change in the biosensing parameters due to DNA orientation within the cavity. For a highly sensitive DNA biosensor like $MoTe_2$ based, it is crucial to consider the DNA interaction with the electrodes in microelectronic environment. We have mainly focused on the impact of such variability from a circuit level perspective. The impact of back-gate bias on the device performance has also been analyzed in details. Lastly, we have considered many orientational structure that has high probability of occurring in real-time experiments. For these cases, the performance of the proposed structure has been analyzed. Hence, this study can be considered as important in the

view that it presents the detailed effect of DNA surface interactions on biosensing performance of highly sensitive $MoTe_2$ based biosensors, which are considered to be next generation biosensors.

Declarations

* **Ethics approval and consent to participate**: Yes

* **Consent for publication:** All authors provide consent for publication.

* **Availability of data and materials:** Data and materials are available upon reasonable request. (mail to corresponding author).

* **Competing interests:** There are no competing interests.

* **Funding:** The authors of this paper would like to acknowledge DST-WB for the financial support. Ref. No: 287 (Sanc.)/ST/P/S&T/6G-43/2017.

* **Authors' contributions**: All authors have contributed equally. All authors participated in reviewing the paper and finalizing the technical content of it.

* **Acknowledgements:** Arpan De will like to thank Dipanjan Sen for valuable discussion in simulation section.

* **Authors' information (optional):** None

Compliance with Ethical Standards section.

* **Disclosure of potential conflicts of interest:** There are no conflict of interests

* **Research involving Human Participants and/or Animals:** Not Applicable

* **Informed consent:** Not Applicable

References

[1] Monika Kundu, P.Krishnan, R.K.Kotnala Gajjala Sumana, "Recent developments in biosensors to combat agricultural challenges and their future prospects," in ScienceDirect, Volume 88, June 2019, Pages 157-178, https://doi.org/10.1016/j.tifs.2019.03.024

[2] Mehrotra, Parikha. “Biosensors and their applications - A review.” Journal of oral biology and craniofacial research vol. 6,2 (2016): 153-9. doi:10.1016/j.jobcr.2015.12.00

[3] S. Kumar, B. Singh and Y. Singh, "Analytical Model of Dielectric Modulated Trench Double Gate Junctionless FET for Biosensing Applications," in IEEE Sensors Journal, vol. 21, no. 7, pp. 8896-8902, 1 April1, 2021, doi: 10.1109/JSEN.2021.3056385.

[4] Ajay, R. Narang, M. Saxena and M. Gupta, "Modeling and Simulation Investigation of Sensitivity of Symmetric Split Gate Junctionless FET for Biosensing Application," in IEEE Sensors Journal, vol. 17, no. 15, pp. 4853-4861, 1 Aug.1, 2017, doi: 10.1109/JSEN.2017.2716102.

[5] Ehsanur Rahman, Abir Shadman, Quazi D.M. Khosru,"Effect of biomolecule position and fill in factor on sensitivity of a Dielectric Modulated Double Gate Junctionless MOSFET biosensor,Sensing and Bio-Sensing Research," in sciencedirect Volume 13, 2017, Pages 49-54,https://doi.org/10.1016/j.sbsr.2017.02.002.

[6] Ehsanur Rahman, Abir Shadman, Quazi D.M. Khosru,"Effect of biomolecule position and fill in factor on sensitivity of a Dielectric Modulated Double Gate Junctionless MOSFET biosensor,Sensing and Bio-Sensing Research," in sciencedirect Volume 13, 2017, Pages 49-54,https://doi.org/10.1016/j.sbsr.2017.02.002.

[7] Chattopadhyay, A., Tewari, S. & Gupta, P.S. Dual-Metal Double-Gate with Low-k/High-k Oxide Stack Junctionless MOSFET for a Wide Range of Protein Detection: a Fully Electrostatic Based Numerical Approach. Silicon 13, 441–450 (2021). https://doi.org/10.1007/s12633-020-00430-4

[8] Kumari, M., Singh, N.K., Sahoo, M. et al. Work function optimization for enhancement of sensitivity of dual-material (DM), double-gate (DG), junctionless MOSFET-based biosensor. Appl. Phys. A 127, 130 (2021). https://doi.org/10.1007/s00339-020-04256-0

[9] Chakraborty, A., Sarkar, A. Analytical modeling and sensitivity analysis of dielectric-modulated junctionless gate stack surrounding gate MOSFET (JLGSSRG) for application as biosensor. J Comput Electron 16, 556–567 (2017). https://doi.org/10.1007/s10825-017-0999-2

[10] Ajay, R. Narang, M. Gupta and M. Saxena, "Investigation of Dielectric-Modulated Double-Gate Junctionless MOSFET for detection of biomolecules," 2013 Annual IEEE India Conference (INDICON), 2013, pp. 1-6, doi: 10.1109/INDCON.2013.6725863.

[11] R. A. Rani and O. Sidek, "ISFET pH sensor characterization: towards biosensor microchip application," 2004 IEEE Region 10 Conference TENCON 2004., 2004, pp. 660-663 Vol. 4, doi: 10.1109/TENCON.2004.1415019.

[12] Shreepriya Das, Haris Vikalo, and Arjang Hassib, "On scaling laws of biosensors: A stochastic approach," Journal of Applied Physics 105, 102021 (2009); https://doi.org/10.1063/1.3116125

[13] Adam Bolotsky et al., "Two-Dimensional Materials in Biosensing and Healthcare: From In Vitro Diagnostics toOptogenetics and Beyond," in ACS Nano 2019, 13, 9781–9810, DOI: 10.1021/acsnano.9b03632

[14] Labib, M, “Electrochemical Methods for the Analysis of Clinically Relevant Biomolecules,” in Chem. 9001-Rev. 2016, 116,9090. https://doi.org/10.1021/acs.chemrev.6b00220

[15] Chekin, F. et al, “Nucleic Aptamer Modified Porous Reduced Graphene Oxide/MoS2 Based Electrodes for Viral Detection: Application to Human

Papillomavirus (HPV),” in Sens. Actuators, B 2018, 262,1000. https://doi.org/10.1016/j.snb.2018.02.065

[16] Hwang, M.T. et al., “Ultrasensitive detection of nucleic acids using deformed graphene channel field effect biosensors,” Nat Commun 11, 1543 (2020). https://doi.org/10.1038/s41467-020-15330-9

[17] Balendhran, S., Walia, S., Nili, H., Ou, J.Z., Zhuiykov, S., Kaner, R.B., Sriram, S., Bhaskaran, M. and Kalantar-zadeh, K. (2013), “Two-Dimensional Molybdenum Trioxide and Dichalcogenides,” in Adv. Funct. Mater., 23: 3952-3970. https://doi.org/10.1002/adfm.201300125

[18] Zhihong Feng et al , “Highly sensitive MoTe2 chemical sensor with fast recovery rate through gate biasing,” in 2D Mater. 4 025018, 2017 .

[19] A. Bhattacharyya, M. Chanda and D. De, "Analysis of Partial Hybridization and Probe Positioning on Sensitivity of a Dielectric Modulated Junctionless Label Free Biosensor," in IEEE Transactions on Nanotechnology, vol. 19, pp. 719-727, 2020, doi: 10.1109/TNANO.2020.3025544.

[20] ATLAS User’s Manual, Silvaco Inc., Santa Clara, CA, USA, 2015.

[21] K. Tamersit, F. Djeffal, Carbon nanotube field-effect transistor with vacuum gate dielectric for label-free detection of DNA molecules: a computational investigation, IEEE Sensor. J. 19 (2019) 9263–9270,https://doi.org/10.1109/JSEN.2019.2925597.

[22] S. Kalra, M. J. Kumar and A. Dhawan, "Dielectric-Modulated Field Effect Transistors for DNA Detection: Impact of DNA Orientation," in IEEE Electron Device Letters, vol. 37, no. 11, pp. 1485-1488, Nov. 2016, doi: 10.1109/LED.2016.2613110

[23] S. O. Kelley, J. K. Barton, N. M. Jackson, L. D. McPherson, A. B. Potter, E. M. Spain, M. J. Allen, and M. G. Hill, “Orienting DNA helices on gold using applied electric fields,” Langmuir, vol. 14, no. 24, pp. 6781–6784, Nov. 1998.

[24] Z.-L. Zhang, D.-W. Pang, R.-Y. Zhang, J.-W. Yan, B.-W. Mao, and Y.-P. Qi, “Investigation of DNA Orientation on Gold by EC- STM,” Bioconjugate Chem., vol. 13, no. 1, pp. 104–109, 2002.

Figures

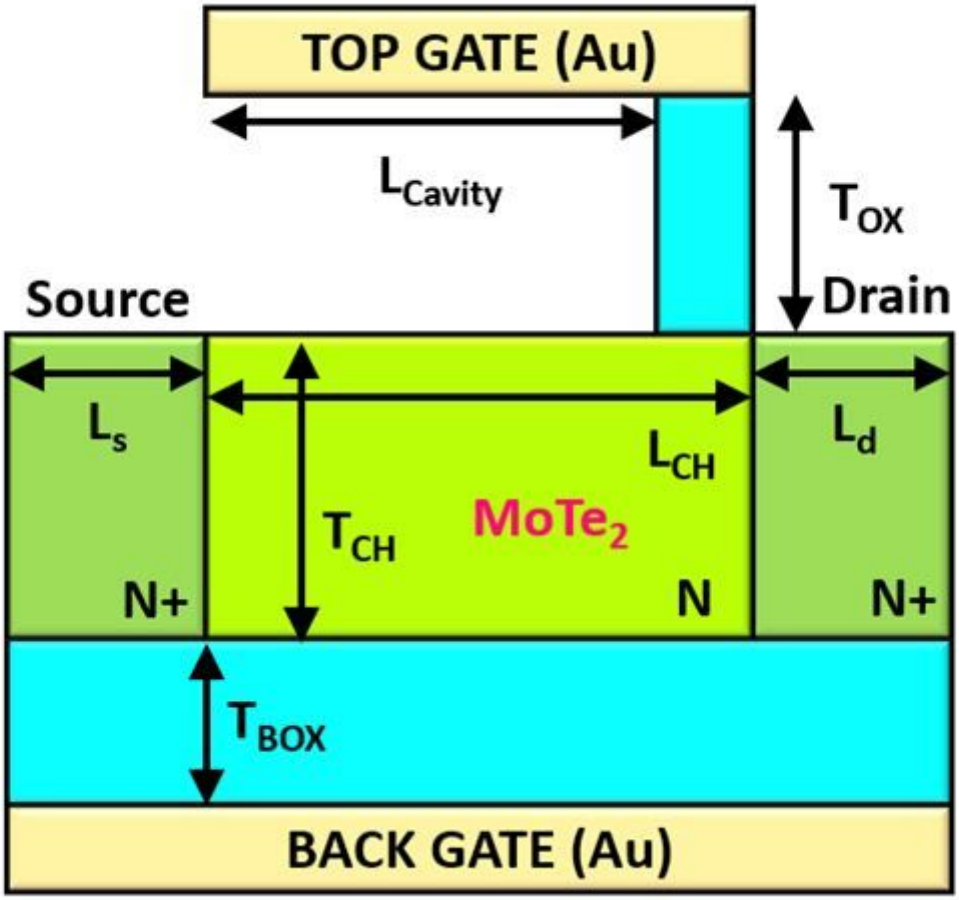

Figure 1

Device Schematic of the proposed MoTe2 AMFET

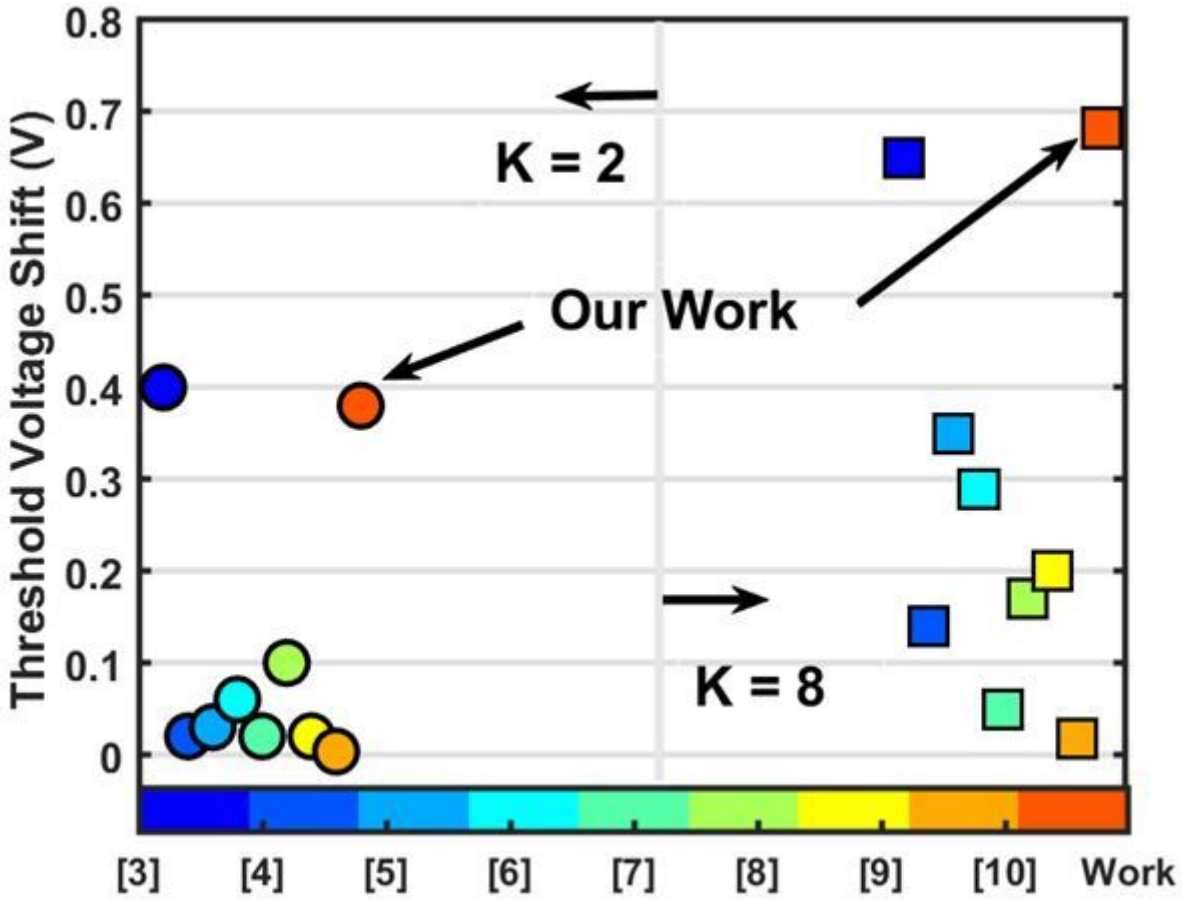

Figure 2

Benchmarking the performance of proposed MoTe2 AMFET with the previously reported studies.

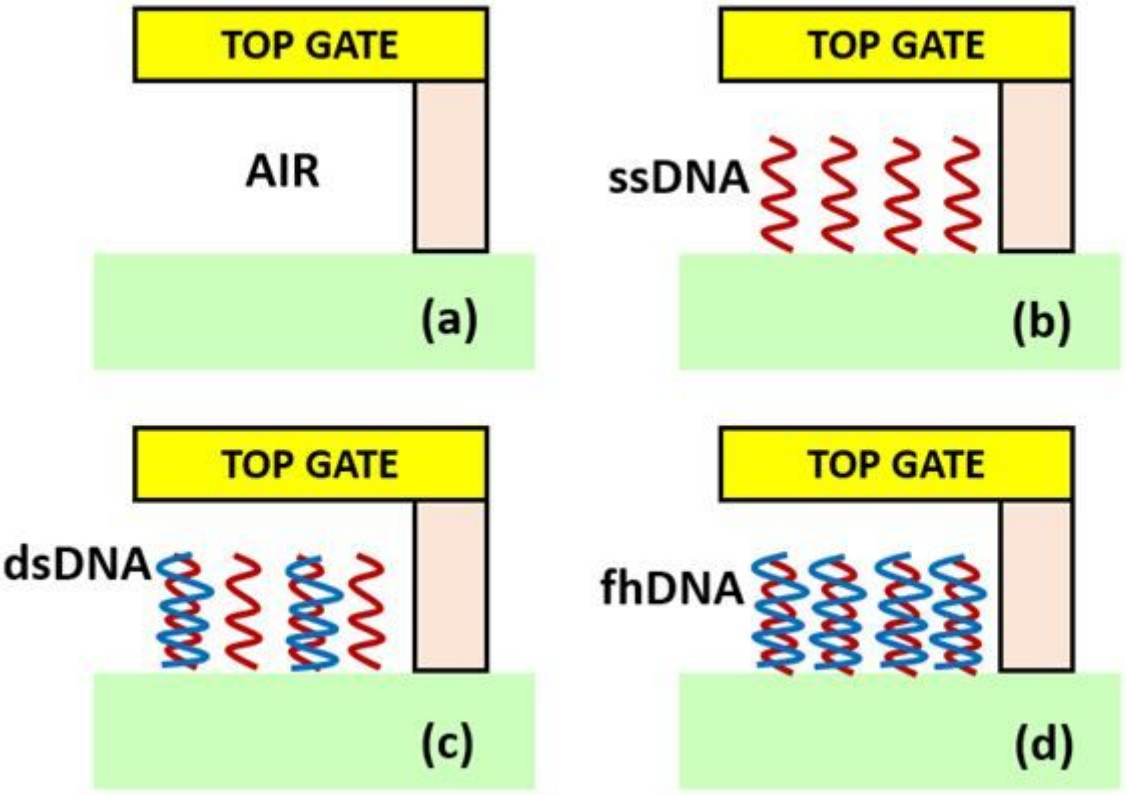

Figure 3

(a) Empty Cavity Condition / Bare Device without DNA immobilized. (b) Genetically coded ssDNA layer formation (c) Intermediate Partial Hybridization of DNA (d) Complete Hybridization of DNA within the cavity.

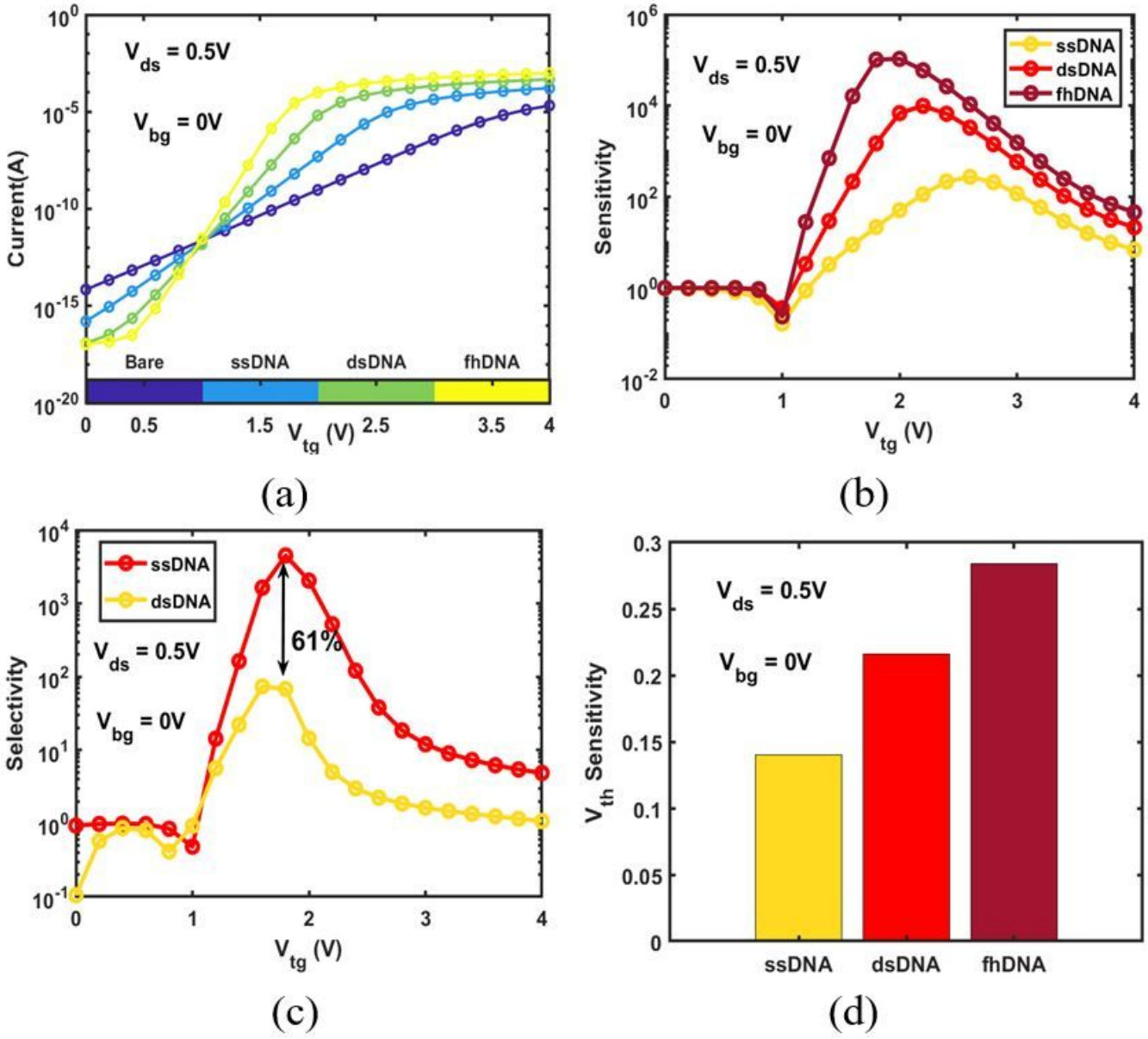

Figure 4

(a) Current profile for the four different stages mentioned in Fig. 3 for different top gate bias (b) The current sensitivity for last three stages with respect to bare device (c) Selectivity of Complete Hybridization Stage with respect to ssDNA and dsDNA (partial hybridization) (d) The threshold voltage sensitivity for the last three stages.

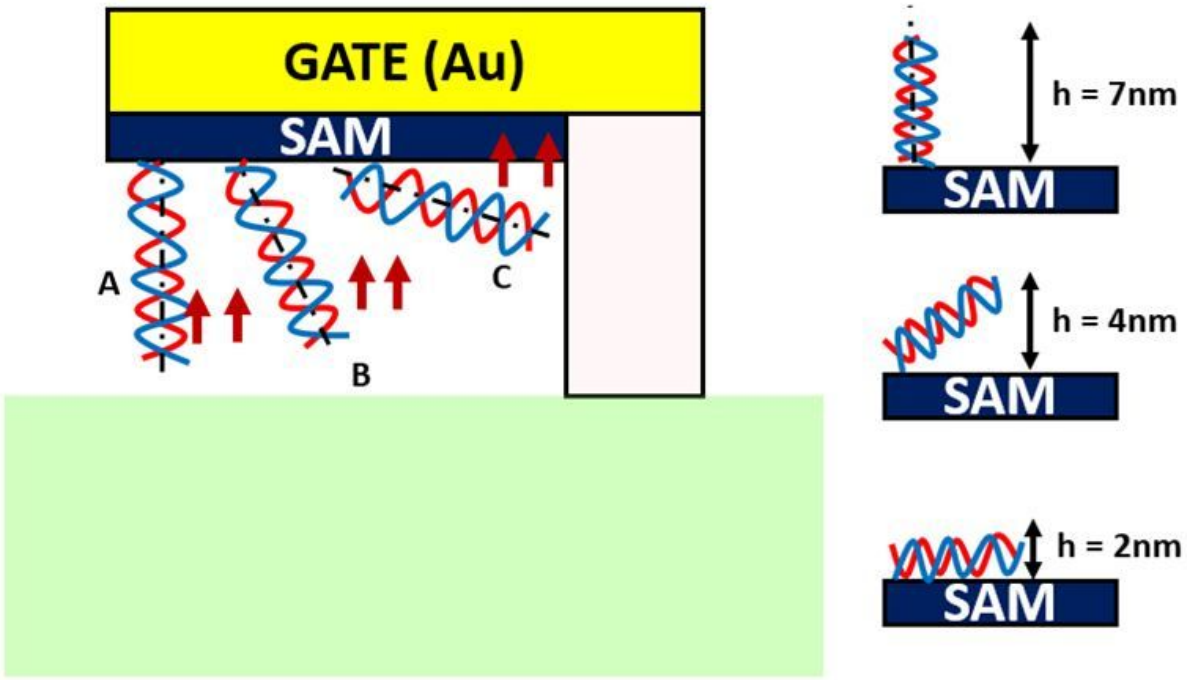

Figure 5

Device Schematic showing the concept of DNA orientation.

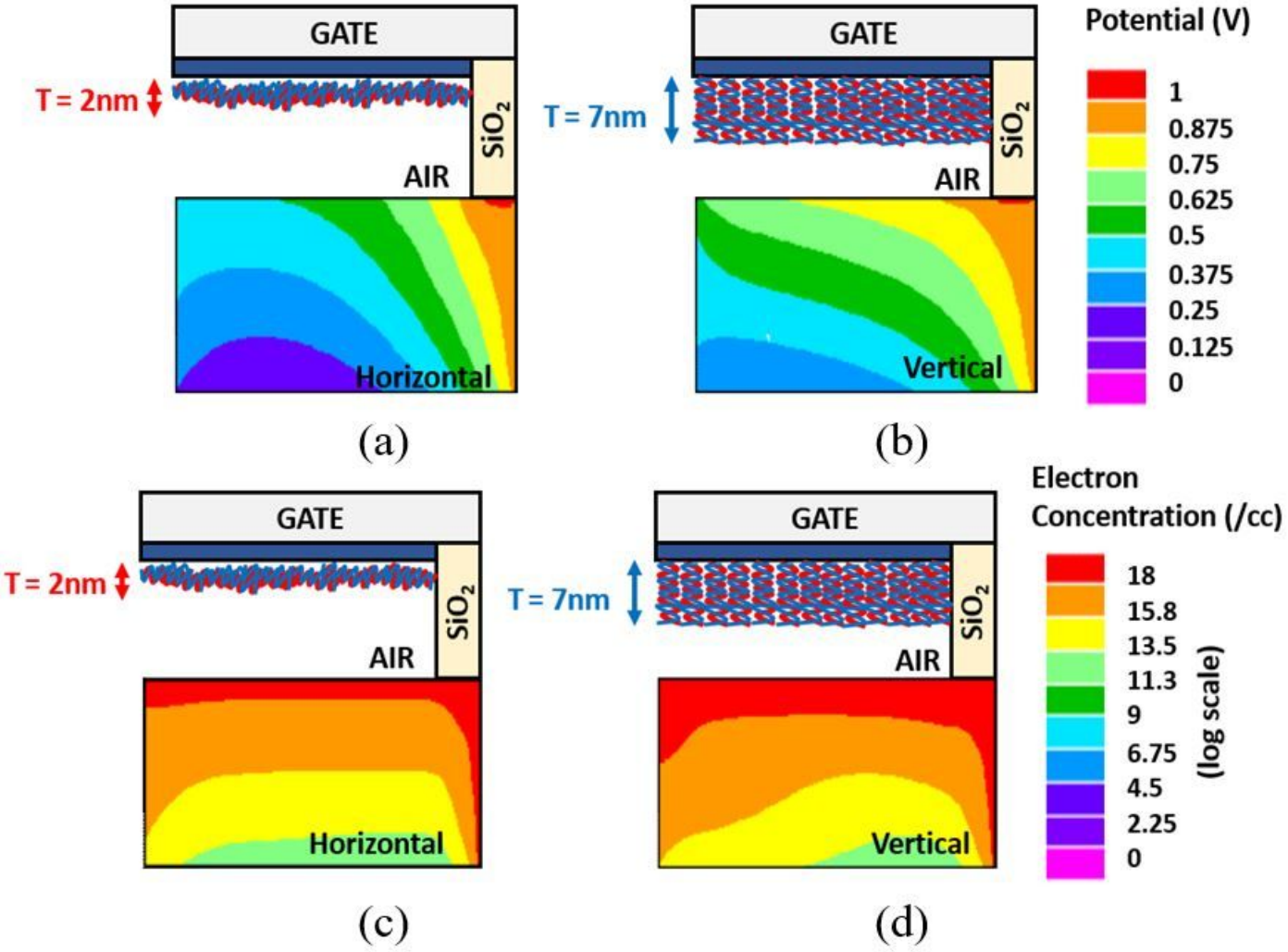

Figure 6

Contour plots for potential distribution and electron concentration in the channel of the proposed device for Horizontal Condition i.e., all DNA make zero degree with SAM layer (a,c) and Vertical Condition i.e., all DNA are perfectly straight (b,d).

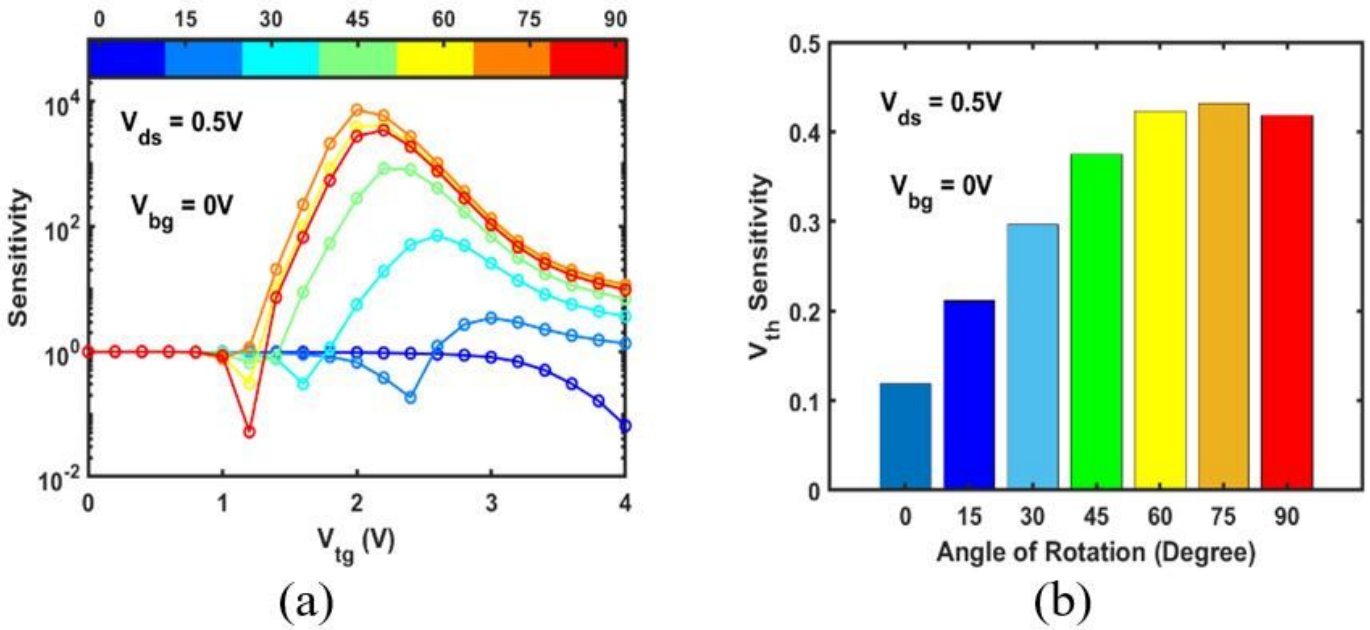

Figure 7

(a) The Current sensitivity of different orientation (based on angle of rotation) with the color bar at the top showing the angle of orientations (in degree) (b) The Threshold Voltage Sensitivity of different angles of orientation of DNA strands.

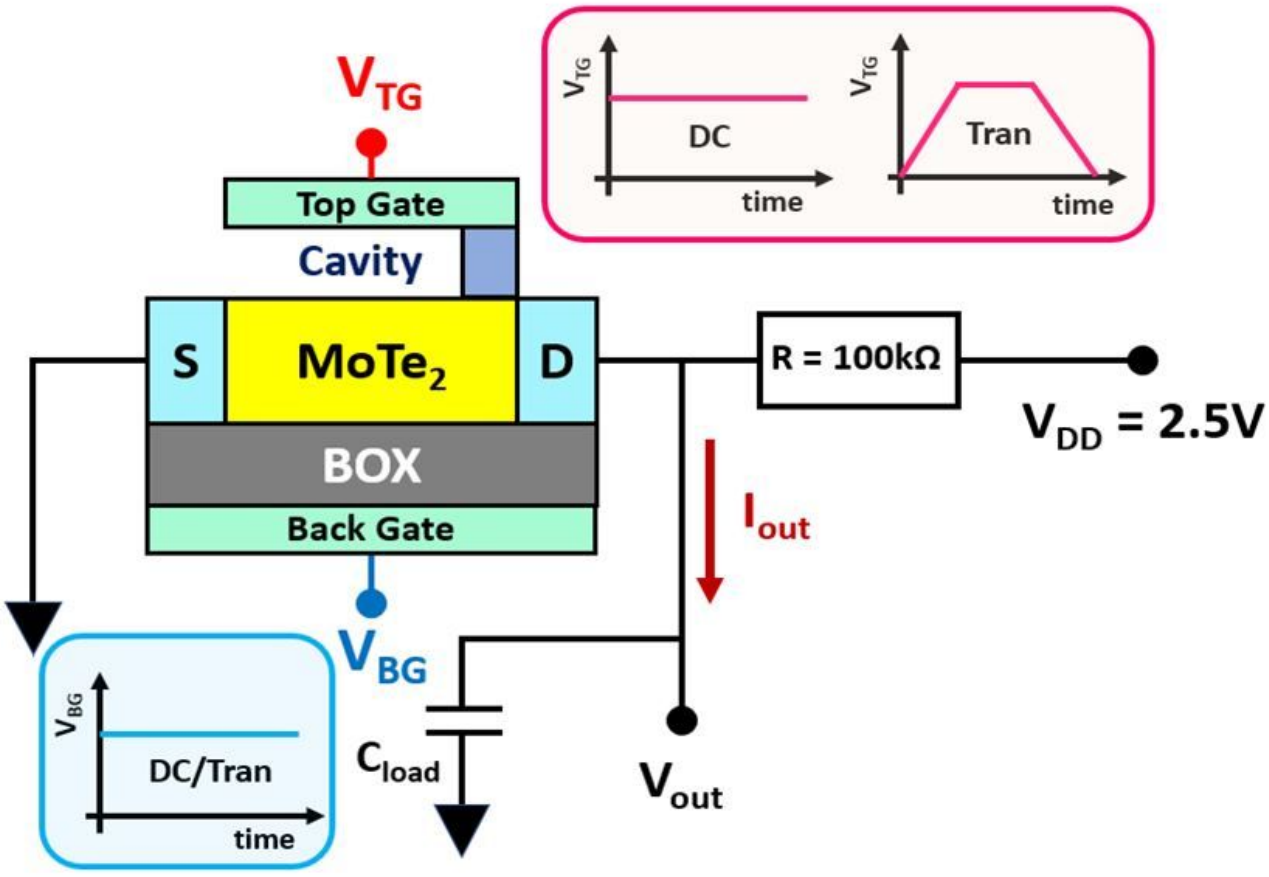

Figure 8

The resistive-load NMOS inverter Circuit proposed for studying the orientation effect on performance of the MoTe2 based AMFET biosensor. The lumped parameters include a load resistance and capacitance. The driver voltage is 2.5V. The Top Gate voltage (VTG) is varied differently for DC and Transient simulations while Back Gate Voltage is considered constant.

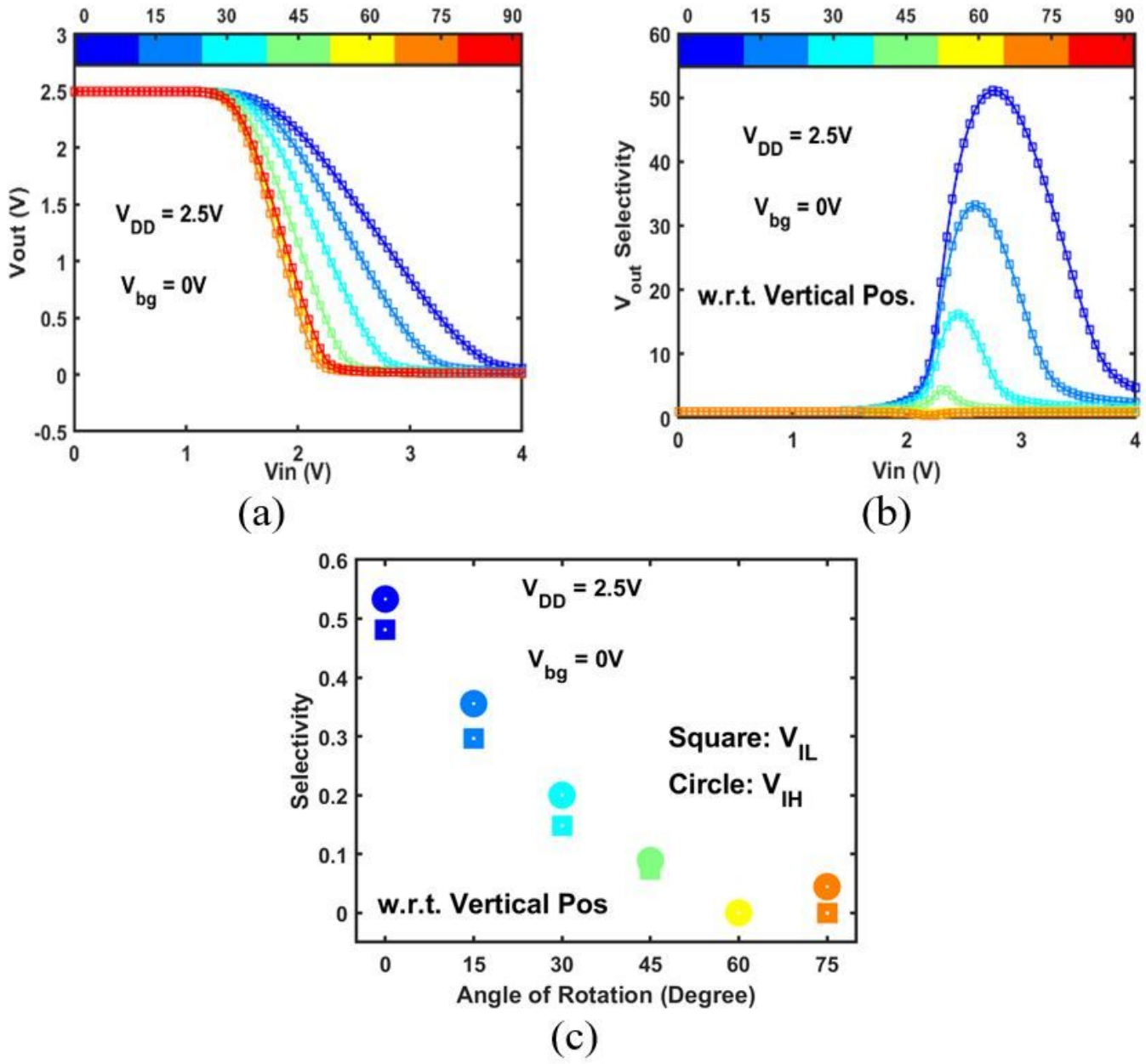

Figure 9

(a) 'Voltage Transfer Characteristics' of the NMOS inverter for different orientation angles. The color bar at the top shows the orientation angles. (b) The selectivity of the Output Voltage (c) Input Low and Input High voltages with respect to the vertical orientation.

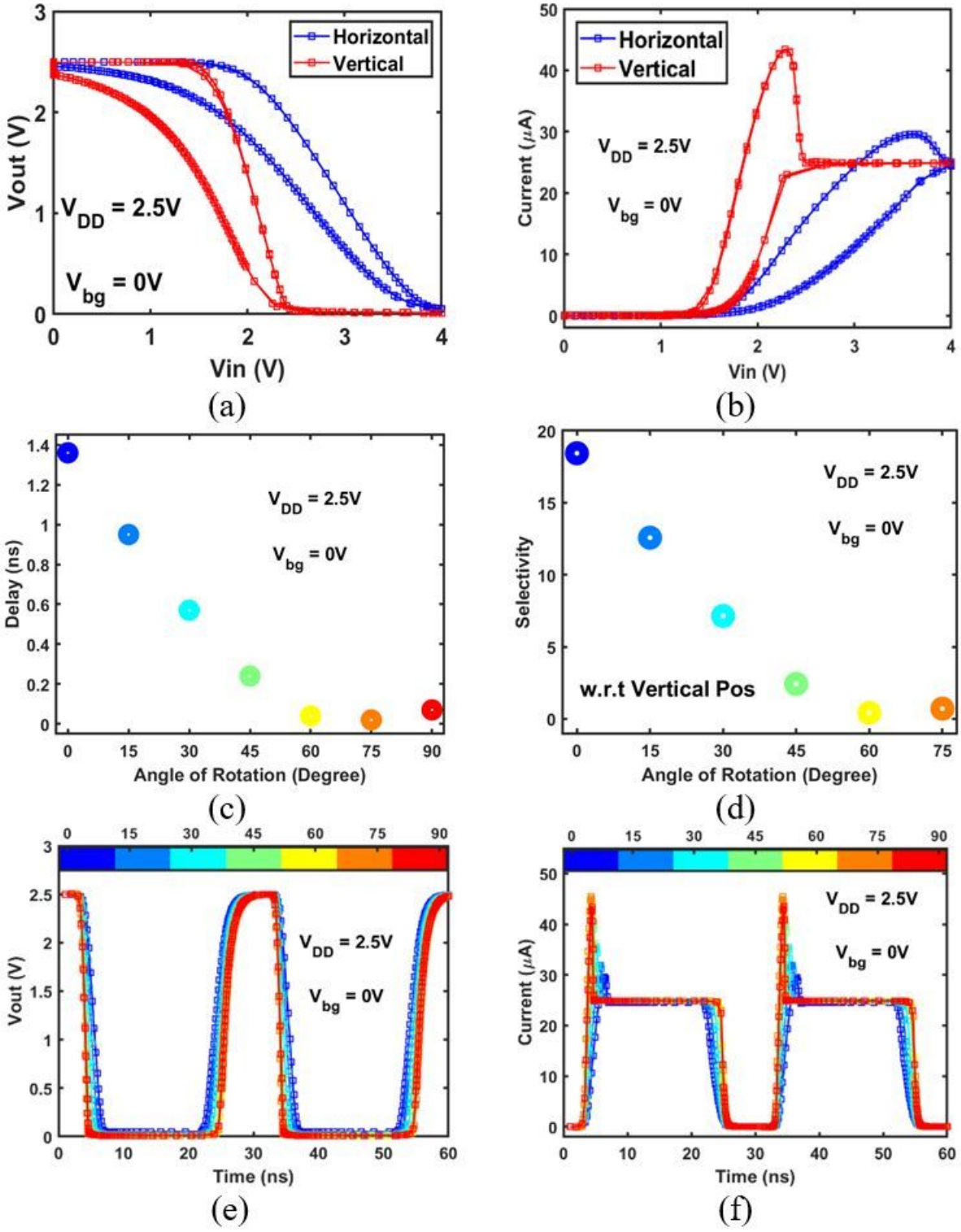

Figure 10

(a) Input-Output Voltage Curve (b) Current-Voltage Profile for the transient simulations with horizontal orientation in blue and vertical orientation in red. (c) Propagation Delay variation of the NMOS inverter with different orientations (d) Selectivity of Delay of all orientations with respect to Vertical Orientation (e) Transient Output Profile for all orientation (f) Transient Current Profile for all orientation (The color bar shows orientation angle in degree).

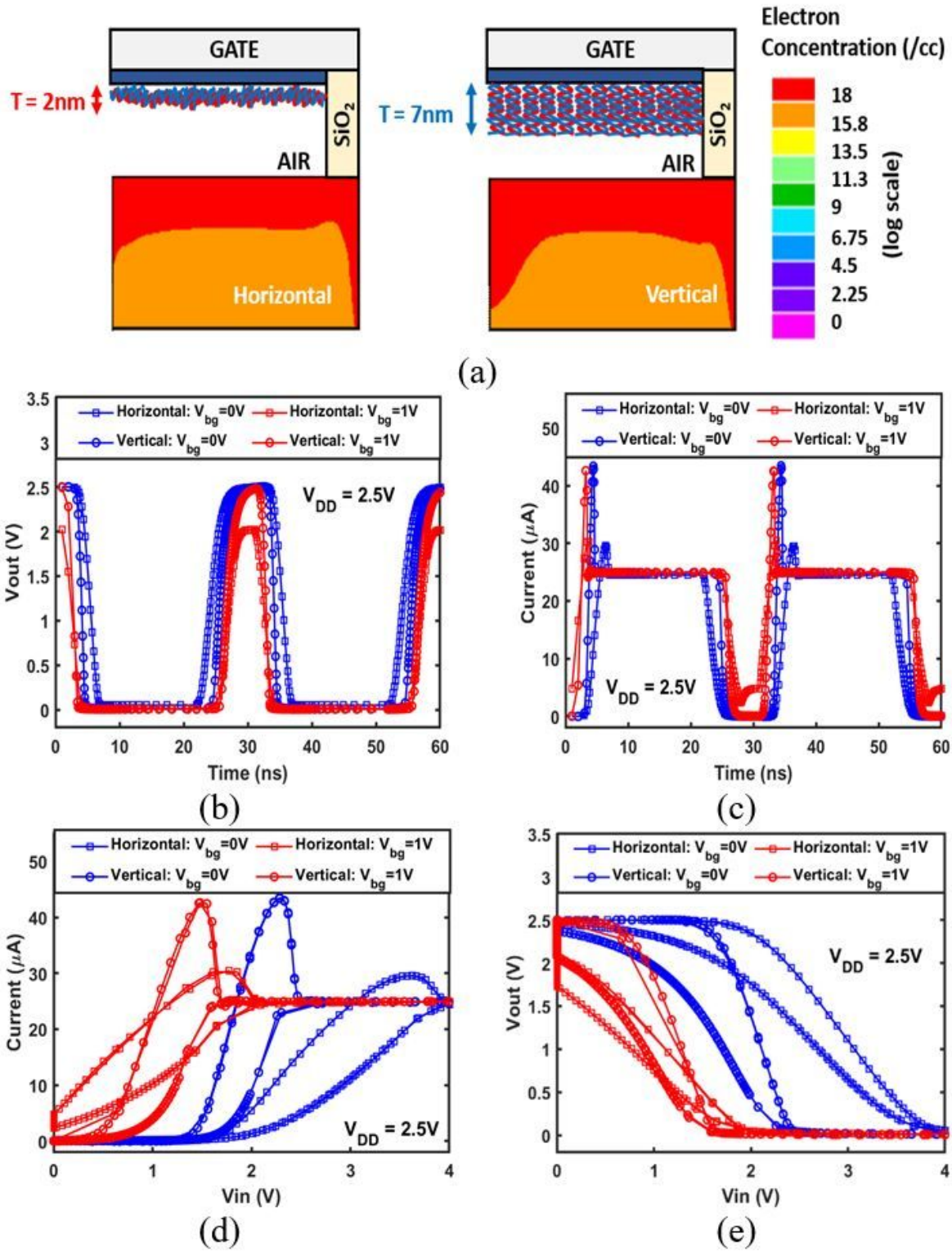

Figure 11

(a) The electron Distribution in the channel in Horizontal and Vertical Condition for a back gate bias of 1V. Transient Curves for (b) Output Voltage and (c) Output Current for back-gate voltage of 1V (red) and 0V (blue) for Horizontal (square) and Vertical (circle) orientations. The (d) Current and (e) Output voltage profiles with input voltages for back-gate voltage of 1V (red) and 0V (blue) for 0V (blue) for Horizontal (square) and Vertical (circle) orientations.

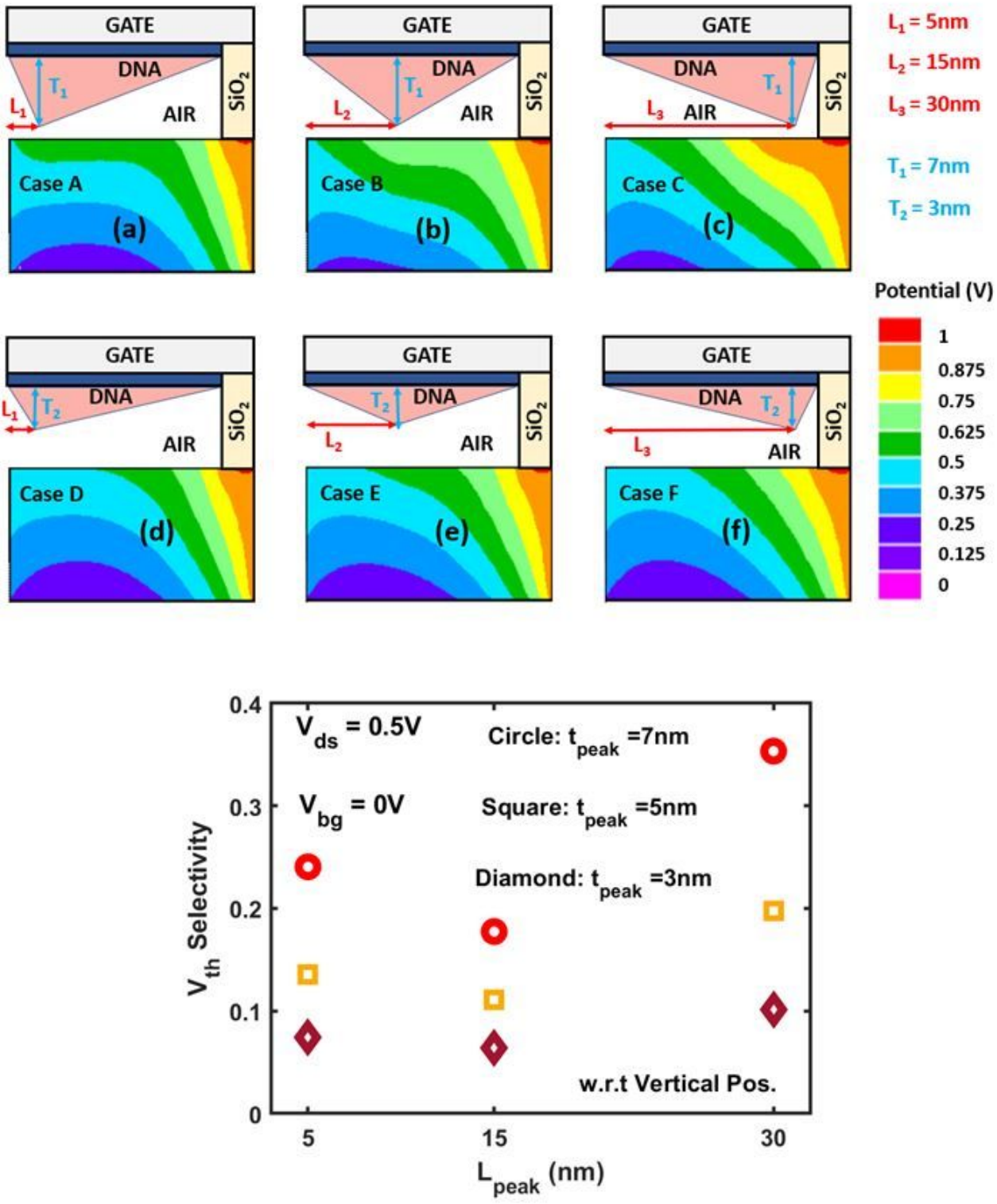

Figure 12

(TOP) The Potential Profile Map for the channel with different DNA layer profiles for (a) Case A (b) Case B (c) Case C (d) Case D (e) Case E (f) Case F. The Top row presents the cases with peak DNA layer thickness of 7nm and the bottom row is for peak DNA layer thickness of 3nm. (BOTTOM) The Threshold voltage selectivity with respect to the vertical orientation with a flat end line of the DNA layer.